

Unexpected reactivity related to support effects during xylose hydrogenation over ruthenium catalysts

Léa Vilcoq,^{*,a} Ana Maria Paez,^a Victoria D. S. Freitas,^a Laurent Veyre,^a Pascal Fongarland,^a and Régis Philippe^a

^a Catalysis, Polymerisation, Processes, Materials (CP2M), UMR 5128 - CNRS, Université Claude-Bernard Lyon 1, CPE-Lyon, F-69616, VILLEURBANNE, France

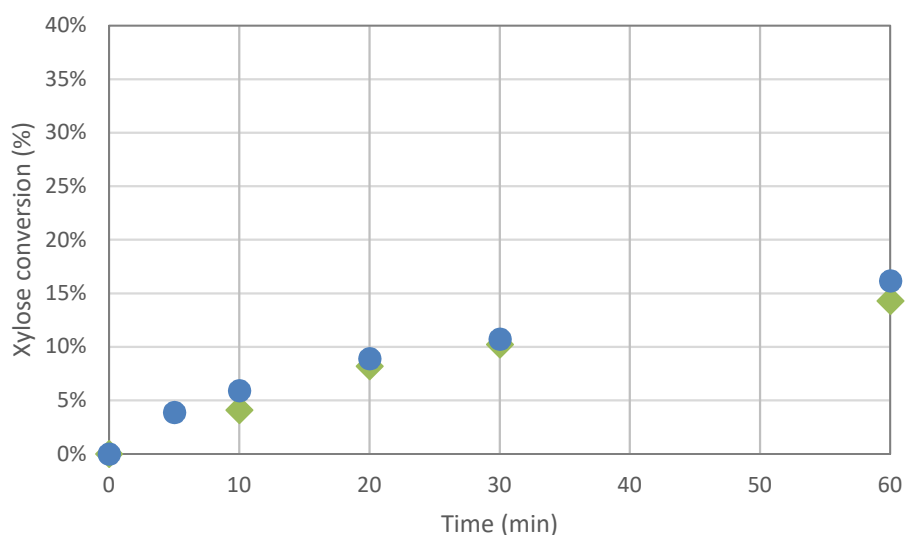
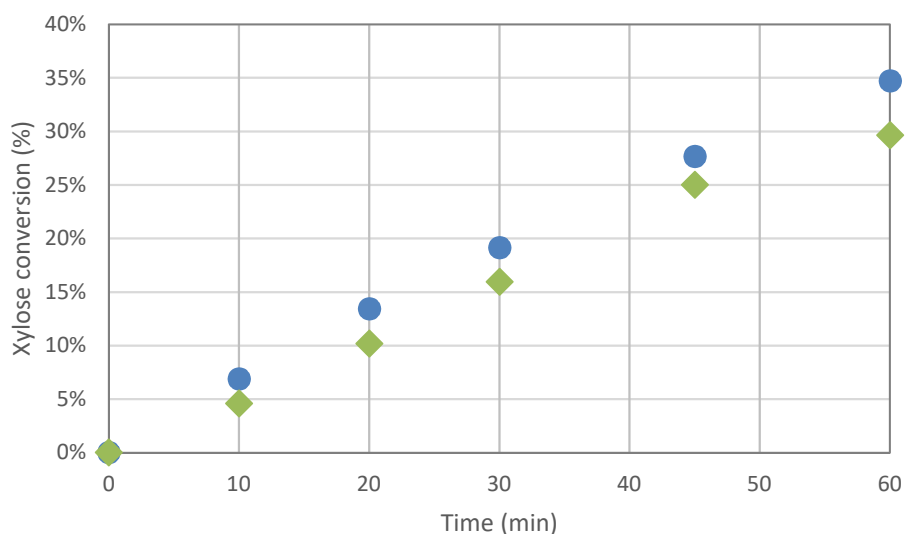
Electronic Supplementary Information

Summary

| | |
|--|----|
| 1. Mass transfer limitations..... | 2 |
| 2. Typical chromatograms of xylose hydrogenation products..... | 4 |
| 3. Kinetics of sugars hydrogenation | 5 |
| 4. Carbon balance..... | 8 |
| 5. XRD diffractograms of TiO ₂ supports..... | 9 |
| 6. N ₂ physisorption isotherms | 10 |
| 7. TEM-EDX of Ru/TiO ₂ -R catalyst..... | 11 |

1. Mass transfer limitations

The absence of influence of stirring rate on the reaction rate (Figure S1) shows the absence of external mass transfer limitations in the studied conditions.



b)

Figure S1. Xylose hydrogenation over Ru/TiO₂-R (a) and Ru/TiO₂-A (b) at different stirring rates (blue circles: 1600 rpm; green squares: 800 rpm). Reaction conditions: 120°C, 40 bar H₂, 0.33 M xylose, ratio Ru/xylose 0.45%.

The resistance of mass transfer inside the catalyst particle was determined through the calculation of Weisz-Prater criterion: (Weisz & Prater, 1954)

$$\phi' = \frac{\bar{r}_p \times L^2}{D_e \times C^*} \quad (S1)$$

With the following values:

Table S1. Values used for Weisz-Prater calculations.

| Parameter | Description | Value (Ru/TiO ₂ -R) | Value (Ru/TiO ₂ -A) |
|-------------|---|--------------------------------|--------------------------------|
| \bar{r} | Apparent rate of reaction (mol.s ⁻¹ .m ⁻³ _{cat}) Calculated from linear regression of data presented on Figure 1 between 0 and 60 min. Catalyst density was assumed to be 4 g.mL ⁻¹ (supplier data) for TiO ₂ -R (...) | 14.78 | 1.59 |
| L | Characteristic length of catalyst grain (m). Calculated as $d_p/6$. | 3.95.10 ⁻⁷ | 1.16.10 ⁻⁷ |
| $D_{e,xy}$ | Effective diffusion coefficient for xylose (m.s ⁻¹). Calculated from $D_e = \frac{\beta_p}{\tau_p} \times D$ | 1.43.10 ⁻¹⁰ | 1.43E-10 |
| D_{e,H_2} | Effective diffusion coefficient for H ₂ (m ² .s ⁻¹). (<i>idem</i>) | 2.58.10 ⁻⁹ | 2.58E-09 |
| β_p | Porosity of catalyst particle (volume ratio). Average value for mesoporous oxide catalyst. | 0.5 | |
| τ_p | Tortuosity of catalyst particle. Average value for mesoporous oxide catalyst. | 3 | |
| D_{xy} | Diffusion coefficient of xylose in water at 120°C (m ² .s ⁻¹). Extrapolated from data from (Mogi et al., 2007) | 8.60.10 ⁻¹⁰ | |
| D_{H_2} | Diffusion coefficient of H ₂ in water at 120°C (m ² .s ⁻¹). Calculated from data from (Verhallen et al., 1984) | 3.42.10 ⁻⁹ | |
| $C_{H_2}^*$ | Concentration of H ₂ in aqueous solution at thermodynamic equilibrium (mol.m ⁻³ _{liq}) Data from (Wisniak et al., 1974), at 120°C, 0.5 M xylose, 400 psig. | 28.58 | |
| C_{xy}^* | Initial concentration of xylose (mol.m ⁻³ _{liq}) | 328.1 | |

The following results were obtained:

Table S2. Results of Weisz-Prater criterion calculation.

| ϕ' | Ru/TiO ₂ -R | Ru/TiO ₂ -A |
|----------------------|------------------------|------------------------|
| Xylose | 0.00489 % | 0.459 % |
| H₂ | 0.00312 % | 0.290 % |

All values are inferior to 30%, therefore satisfying the Weisz-Prater criterion and demonstrating the absence of internal mass transfer limitations.

References

- Mogi, N., Sugai, E., Fuse, Y., & Funazukuri, T. (2007). Infinite dilution binary diffusion coefficients for six sugars at 0.1 MPa and temperatures from (273.2 to 353.2) K. *Journal of Chemical and Engineering Data*, 52(1), 40–43. <https://doi.org/10.1021/je0601816>
- Verhallen, P. T. H. M., Oomen, L. J. P., Elsen, A. J. J. M. v. d., Kruger, J., & Fortuin, J. M. H. (1984). The diffusion coefficients of helium, hydrogen, oxygen and nitrogen in water determined from the permeability of a stagnant liquid layer in the quasi-s. *Chemical Engineering Science*, 39(11), 1535–1541. [https://doi.org/10.1016/0009-2509\(84\)80082-2](https://doi.org/10.1016/0009-2509(84)80082-2)
- Weisz, P. B., & Prater, C. D. (1954). Interpretation of Measurements in Experimental Catalysis. In *Advances in Catalysis* (Volume 6, pp. 143–196). Elsevier. [https://doi.org/10.1016/S0360-0564\(08\)60390-9](https://doi.org/10.1016/S0360-0564(08)60390-9)
- Wisniak, J., Hershkowitz, M., Leibowitz, R., & Stein, S. (1974). Hydrogen Solubility in Aqueous Solutions of Sugars and Sugar Alcohols. *Journal of Chemical and Engineering Data*, 19(3), 247–249. <https://doi.org/10.1021/je60062a008>

2. Typical chromatograms of xylose hydrogenation products

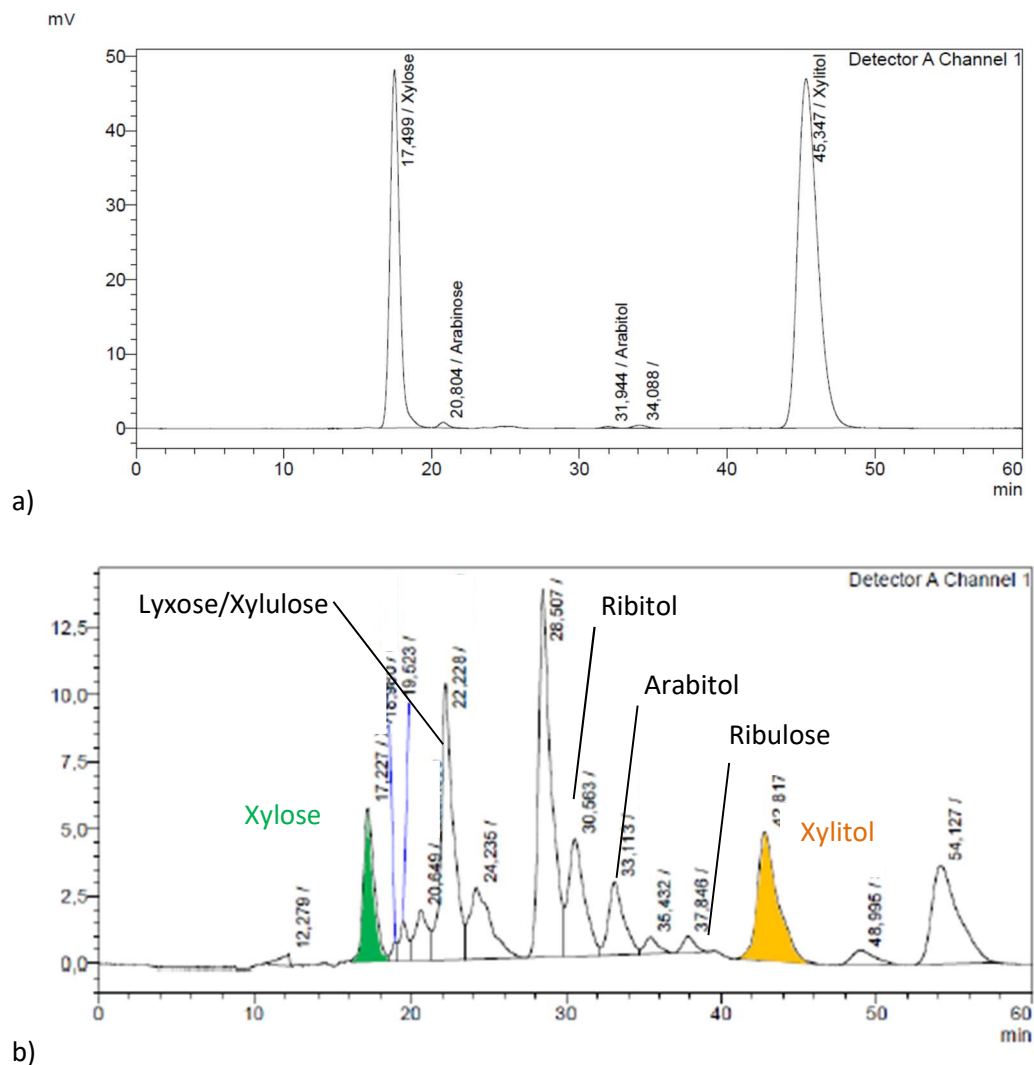


Figure S2. Chromatograms of reaction medium during xylose hydrogenation over a) Ru/TiO_2-R ; b) Ru/TiO_2-A .

3. Kinetics of sugars hydrogenation

The kinetic model was based on the reaction pathway presented in manuscript on Figure 8. In this mechanism, xylose, lyxose, xylulose and ribulose are grouped (“sugars”) and xylitol, arabitol and ribitol are grouped (“polyols”). Sugars are hydrogenated into polyols with the rate of reaction r_H or degraded into unknown products with the rate of reaction r_D . The amount of unknown products corresponds to the loss in carbon balance (equation (S2)).

$$[Unknowns]_t = \sum_{t_0} [Products] - \sum_t [Products] \quad (S2)$$

All concentrations are molar concentrations and the volume of liquid is assumed to be constant during the reaction. The material balance is presented in Equation S3.

$$[Sugars]_0 + [Polyols]_0 = [Sugars]_t + [Polyols]_t + [Unknowns]_t \quad (S3)$$

The rate of hydrogenation is assumed to be first order in Sugars (equation (S4)). Hydrogen concentration is neglected (in experimental conditions, H_2 pressure is constant).

$$r_H V_{liq} = -k_H \times [Sugars]_t \quad (S4)$$

The rate of degradation is assumed to be first order in Sugars (equation (S5)).

$$r_D V_{liq} = -k_D \times [Sugars]_t \quad (S5)$$

A system of ordinary differential equation can be built from (S3), (S4), (S5):

$$\begin{cases} r_{Sugars,t} = \frac{d[Sugars]}{dt} = -(k_H + k_D) \times [Sugars]_t \\ r_{Polyols,t} = \frac{d[Polyols]}{dt} = k_H \times [Sugars]_t \\ r_{Unknowns,t} = \frac{d[Unknowns]}{dt} = k_D \times [Sugars]_t \end{cases} \quad (S6)$$

An analytical solution to the system (S6) and (S3) is presented in (S7):

$$\begin{cases} [Sugars]_t = [Sugars]_0 \times e^{-(k_H+k_D)t} \\ [Polyols]_t = [Polyols]_0 + [Sugars]_0 \times k_H / (k_H + k_D) \times (1 - e^{-(k_H+k_D)t}) \\ [Unknowns]_t = [Sugars]_0 \times k_D / (k_H + k_D) \times (1 - e^{-(k_H+k_D)t}) \end{cases} \quad (S7)$$

This solution was implemented in Excel with the time values used in experiments. k_H and k_D were determined for each catalyst and each temperature by minimizing the function of sum of relative square errors between experimental and modelling results (equation (S8)) using Excel solver (generalized reduced gradient function). An example is presented in Table S3 and Figure 9 in the manuscript.

$$\min_{\hat{\beta}} SSE(\beta) = \sum_{i=1}^n \frac{(y_i - f(x_i, \hat{\beta}))^2}{y_i} \quad (S8)$$

Where SSE is the error sum of squares, y_i the experimental concentration data, $f(x_i, \hat{\beta})$ the analytical solution of the ODE system, i.e., the calculated concentrations as a function of x_i (time, initial

conditions, and temperature), and β the adjusted vector which contains the final estimates of the kinetic parameters.

Table S3. Example of results of kinetic modelling and SSE in comparison with experimental data – catalyst Ru/TiO₂-R, 120°C.

| Experimental data | | | | Modelling data | | | | SSE | | |
|-------------------|------------------------|------------------------|------------------------|----------------|------------------------|------------------------|------------------------|----------|----------|-------------|
| time | [Xylose] | [Xylitol] | Degradation | time | SUGARS | POLYOLS | Degradation | SUGARS | POLYOLS | Degradation |
| (min) | (mol.L ⁻¹) | (mol.L ⁻¹) | (mol.L ⁻¹) | (min) | (mol.L ⁻¹) | (mol.L ⁻¹) | (mol.L ⁻¹) | | | |
| 0 | 0.328 | 0.001 | 0.000 | 0 | 0.328 | 0.001 | 0.000 | - | - | - |
| 10 | 0.270 | 0.061 | 0.000 | 10 | 0.328 | 0.001 | 0.000 | 6.40E-04 | 2.01E-03 | - |
| 20 | 0.214 | 0.116 | 0.000 | 20 | 0.257 | 0.072 | 0.001 | 8.44E-04 | 1.09E-03 | - |
| 30 | 0.166 | 0.164 | 0.000 | 30 | 0.201 | 0.127 | 0.001 | 4.54E-04 | 2.39E-04 | - |
| 60 | 0.059 | 0.271 | 0.000 | 60 | 0.157 | 0.171 | 0.002 | 4.32E-03 | 1.36E-03 | - |
| 120 | 0.000 | 0.326 | 0.003 | 120 | 0.075 | 0.252 | 0.002 | - | 9.00E-04 | 2.47E-08 |
| 180 | 0.000 | 0.327 | 0.003 | 180 | 0.017 | 0.309 | 0.003 | - | 5.21E-05 | 1.57E-05 |
| 240 | 0.000 | 0.326 | 0.003 | 240 | 0.004 | 0.322 | 0.003 | - | 1.06E-06 | 2.88E-05 |

A parity plot was built for each catalyst to compare visually experimental and modelling data. The model fits the experimental data in the range $\pm 10\%$ (Figure S3).

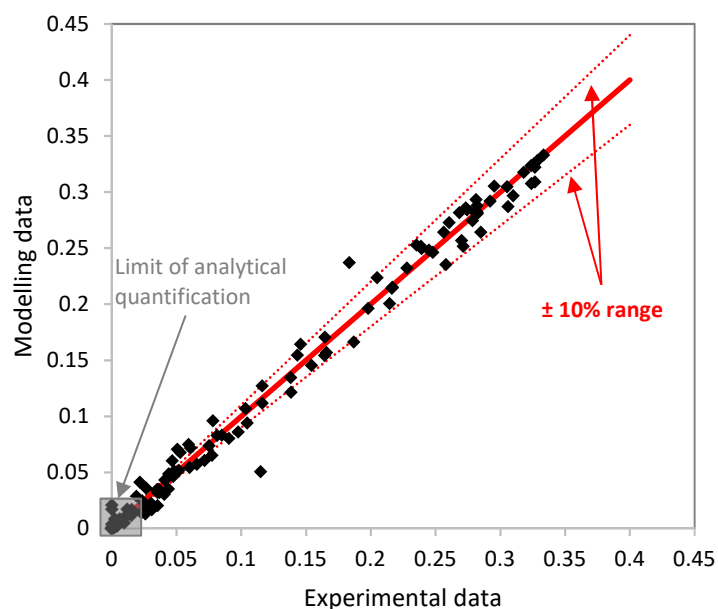


Figure S3. Parity plot for experimental and modelling results (100-140°C, Ru/TiO₂-A and Ru/TiO₂-R).

The calculated values of k_H and k_D at three different temperatures were used to determine energies of activation for hydrogenation and degradation reactions for each catalyst, using the semi-empirical

Arrhenius law (S9). The linear regression of $\ln k$ as a function of $-1/RT^\circ$ gave E_a as slope. Results are presented in Table S4.

$$k = Ae^{-\frac{E_a}{RT}} \Rightarrow \ln k = \ln A - \frac{E_a}{RT} \quad (S9)$$

Turn-Over Frequency (TOF) was calculated from the initial rate of hydrogenation ($t=0$) and the number of ruthenium atoms able to activate H_2 ($n_{Ru,A}$, given by H_2 chemisorption measurements) at $120^\circ C$ (equation (S10)). Results are presented in Table S4 and in Table 3 in the manuscript.

$$TurnOver\ Frequency\ (TOF) = \frac{r_{H,0}}{n_{Ru,A}} = \frac{k_H \times [Sugars]_0 \times V_L}{n_{Ru,A}} \quad (S10)$$

Turn-Over Frequency of degradation reaction (TOF_{DEG}) was calculated from the initial rate of degradation ($t=0$) and the total number of acid sites (n_{H+} , given by H_2 chemisorption measurements) at $120^\circ C$ (equation (S11)). Results are presented in Table 3 in the manuscript.

$$TurnOver\ Frequency\ (TOF) = \frac{r_{D,0}}{n_{H+}} = \frac{k_D \times [Sugars]_0 \times V_L}{n_{H+}} \quad (S11)$$

Table S4. Results of kinetic modelling.

| Catalyst | Temperature (K) | k_H (min^{-1}) | k_D (min^{-1}) | TOF (s^{-1}) | E_{aH} ($kJ.mol^{-1}$) | E_{aD} ($kJ.mol^{-1}$) |
|------------------------|-----------------|----------------------|----------------------|------------------|----------------------------|----------------------------|
| Ru/TiO ₂ -R | 373 | 1.14E-02 | 1.85E-04 | 0.469 | 83.7 | 147.9 |
| | 393 | 2.44E-02 | 2.22E-04 | 0.990 | | |
| | 413 | 1.59E-01 | 2.03E-02 | 5.985 | | |
| Ru/TiO ₂ -A | 373 | 9.57E-04 | 3.87E-04 | 0.036 | 18.5 | 106.2 |
| | 393 | 1.26E-03 | 2.75E-03 | 0.052 | | |
| | 413 | 1.70E-03 | 1.06E-02 | 0.071 | | |

4. Carbon balance

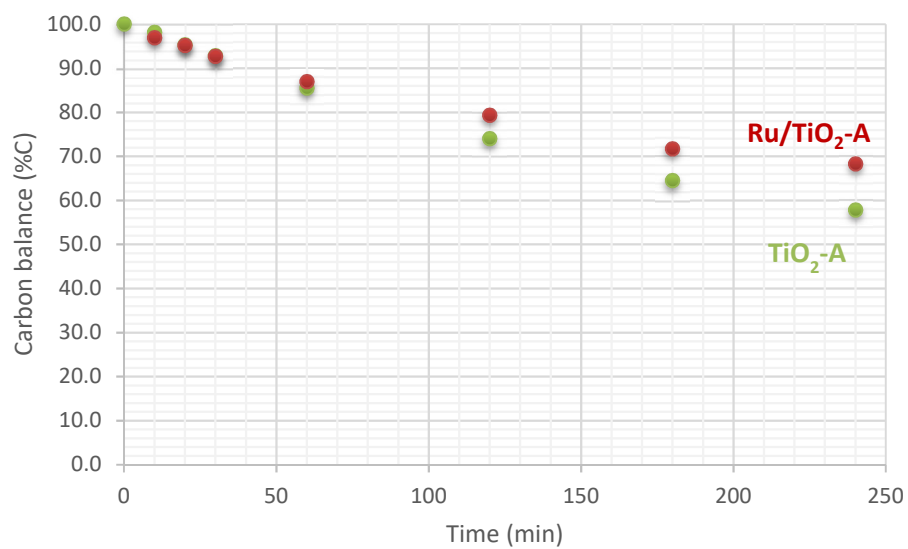


Figure S4. Carbon balance during xylose hydrogenation over Ru/TiO₂-A and TiO₂-A. Reaction conditions: 120°C, 40 bar H₂, 0.33 M xylose, ratio Ru/xylose 0.45%.

5. XRD diffractograms of TiO₂ supports

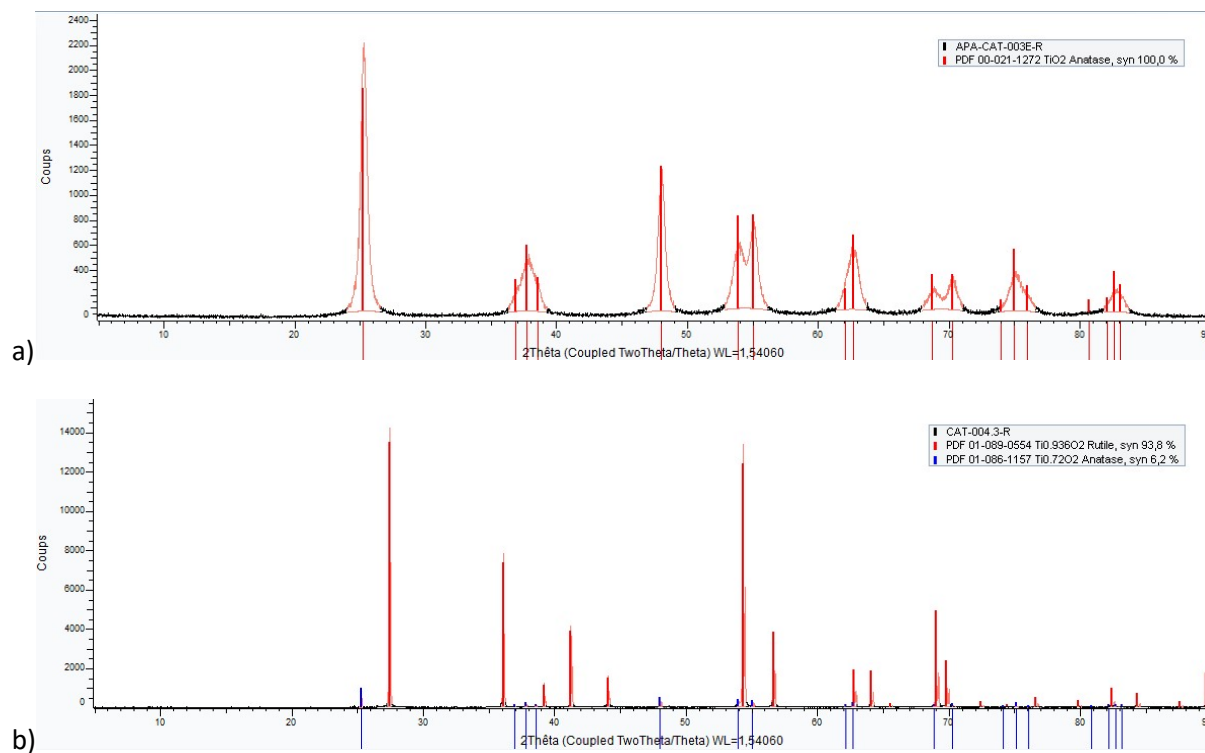


Figure S5. XRD diffractograms and references of Ru/TiO₂-A (a) and Ru/TiO₂-R (b)

6. N₂ physisorption isotherms

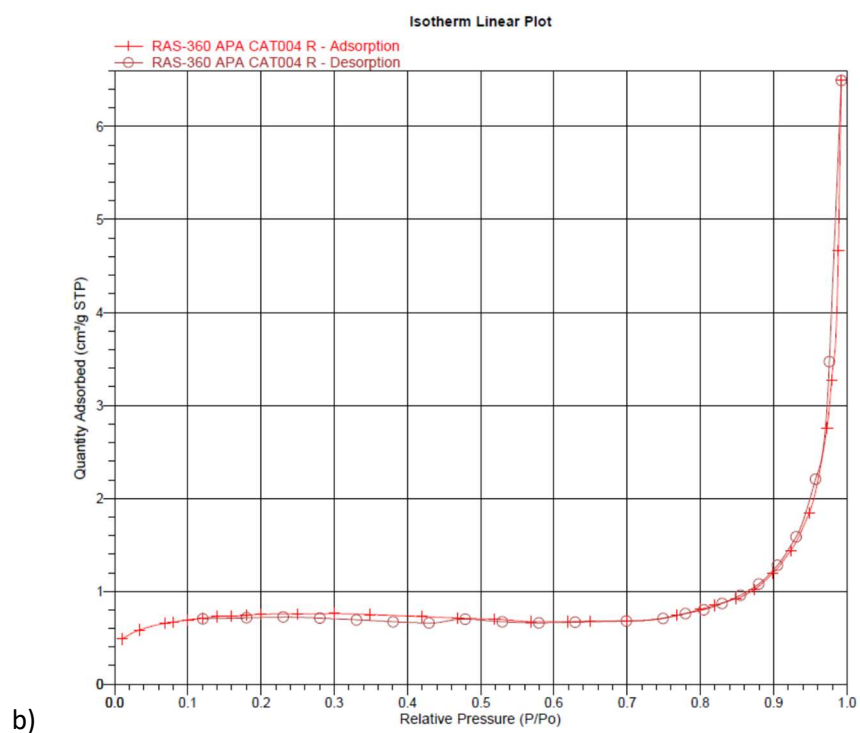
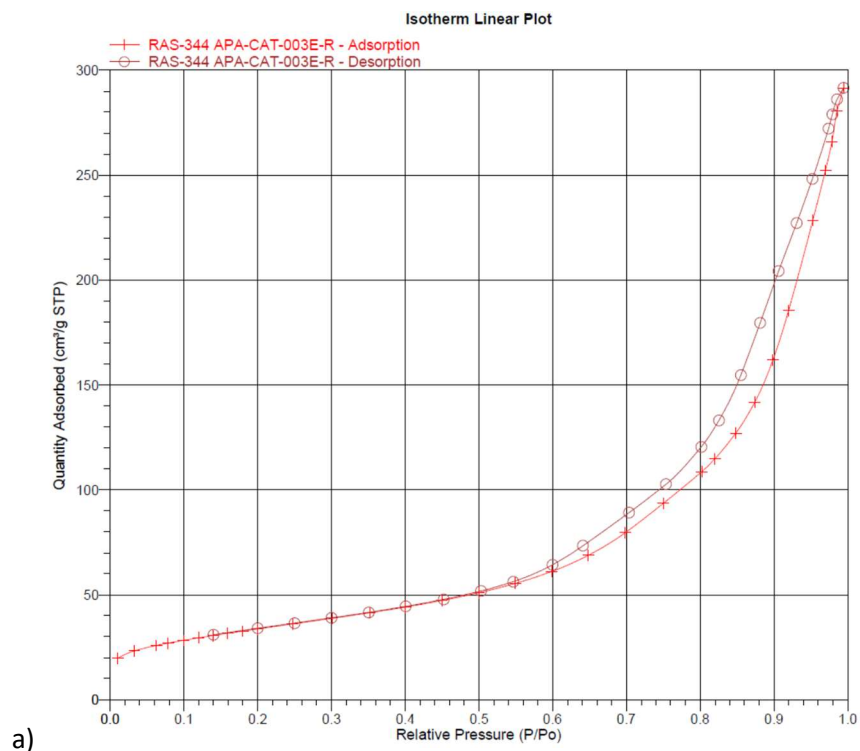


Figure S6. N₂ physisorptions isotherms of Ru/TiO₂-A (a) and RuTiO₂-R (b) catalysts.

7. TEM-EDX of Ru/TiO₂-R catalyst.

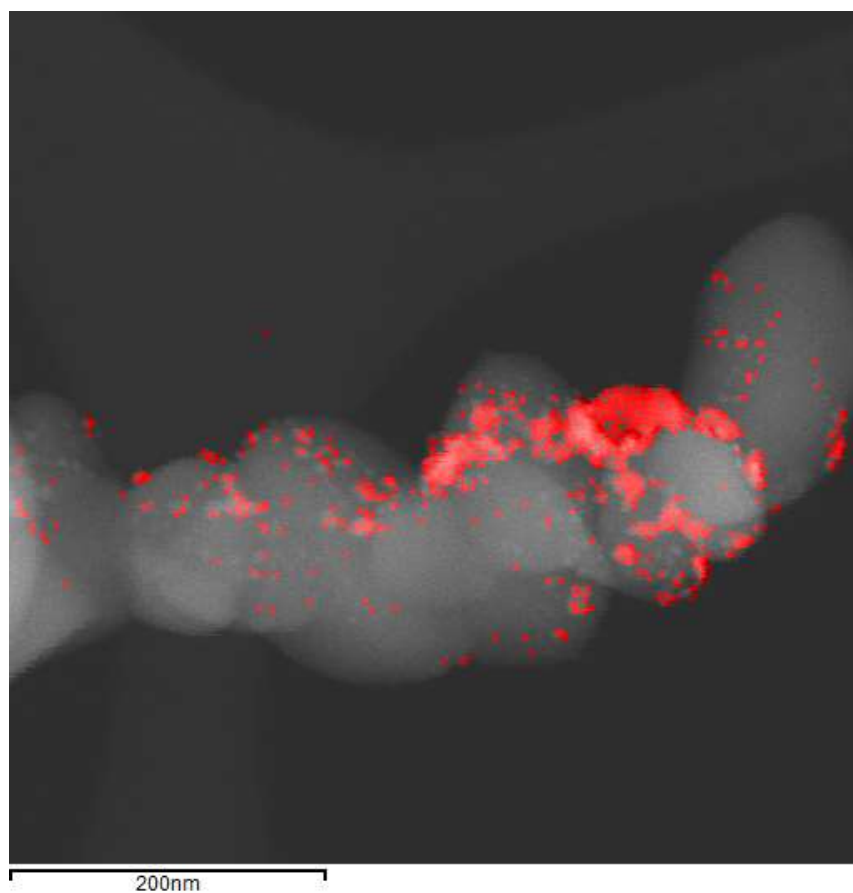


Figure S7. TEM-EDX mapping of Ru on Ru/TiO₂-R catalyst.